

Elucidation of the Magnetism of $[\text{Co}_2\text{PdCl}_2(\text{dpa})_4]$: Origin of a Large Temperature Domain of TIP Behavior

W. Van den Heuvel* and L. F. Chibotaru

Division of Quantum Chemistry and Physical Chemistry, Katholieke Universiteit Leuven, Celestijnenlaan 200F, B-3001 Leuven, Belgium

Received January 5, 2009

The recently synthesized heterotrimetallic complex $[\text{Co}_2\text{PdCl}_2(\text{dpa})_4]$ shows an unusual temperature-independent paramagnetism (TIP), extending over the whole experimental temperature range (0–300 K; Rohmer et al. *Angew. Chem., Int. Ed.* **2007**, 46, 3533). We explain this behavior from a microscopic approach, using ligand-field theory and Anderson's kinetic exchange theory, treating the nonmagnetic Pd^{II} as a ligand. The orbital degeneracy of the Co^{II} ions is taken into account in the construction of the model Hamiltonian. The extension of the TIP behavior, compared to that of mononuclear Co^{II} compounds, over the whole temperature domain, is explained by the quenching of magnetic moments in thermally populated levels by a strong antiferromagnetic exchange interaction.

1. Introduction

Anisotropic magnetic properties of transition-metal complexes have attracted increasing interest in the last years, mostly in connection with the design of efficient single-molecule magnets.² Among molecular compounds exhibiting strong magnetic anisotropy, those containing Co^{II} ions present us with problems defying understanding in terms of simple spin Hamiltonians, which have been very successful in the field of molecular magnetism. Today, the possibilities of Co^{II} ions in the search for materials with desired magnetic properties are explored intensively. Theoretical investigations into the nature of the magnetic behavior of such compounds are therefore very desirable, in particular for pointing out the limitations of the simple spin Hamiltonians.

This paper deals with the theoretical analysis of the magnetism of the recently synthesized heterotrimetallic complex $[\text{Co}_2\text{PdCl}_2(\text{dpa})_4]$.¹ In this complex, the two magnetic Co^{II} ions are separated by and are collinear with the nonmagnetic Pd^{II} ion. They are held together by four dpa ligands and two Cl^- ions, forming a complex with D_4 symmetry (Figure 1). The coupling between the Co^{II} ions was shown to be antiferromagnetic and stronger than that in any preceding Co^{II} dinuclear complex.¹ The magnetic susceptibility of this complex is almost temperature-independent from 0 to 300 K, as follows from the linear behavior of χT (Figure 5).¹ The

explanation of this behavior will be the subject of the present paper.

To analyze experimental data theoretically, exchange interactions between transition-metal ions with local anisotropies are usually modeled with a spin Hamiltonian, working in the local spin states. For example, when the local symmetry is tetragonal around the local z axis, one uses

$$\hat{H} = \sum_{i,j} J_{ij} \hat{S}_i \cdot \hat{S}_j + \sum_i D_i \hat{S}_{iz}^2 \quad (1)$$

Inherent in this Hamiltonian are the assumptions that the local ground states are not orbitally degenerate and that spin–orbit coupling can be accounted for by second-order perturbation theory. In a (distorted) octahedral ligand field, high-spin Co^{II} ($S = 3/2$) does not belong to this class of systems because of its 3-fold orbital (quasi)degeneracy, leading to unquenched orbital momentum in the ground state, together with a relatively strong spin–orbit coupling constant ($\zeta \approx 500 \text{ cm}^{-1}$). This makes the actual situation far from the pure spin limit, and a more detailed Hamiltonian is called for.

The theoretical framework for the study of exchange-coupled transition-metal ions is already established: it consists of a combination of ligand-field theory and Anderson's kinetic exchange theory.³ In the case of orbitally degenerate ions, the exchange interaction is described by a spin–orbital Hamiltonian, which is, in general, anisotropic.^{4,5} In the context of molecular magnetism, spin–orbital exchange

*To whom correspondence should be addressed. E-mail: willem.vandenheuvel@chem.kuleuven.be.

(1) Rohmer, M.-M.; Liu, I. P.-C.; Lin, J.-C.; Chiu, M.-J.; Lee, C.-H.; Lee, G.-H.; Bénard, M.; López, X.; Peng, S.-M. *Angew. Chem., Int. Ed.* **2007**, 46, 3533.

(2) Gatteschi, D.; Sessoli, R.; Villain, J. *Molecular Nanomagnets*; Oxford University Press: Oxford, U.K., 2006.

(3) Anderson, P. W. *Phys. Rev.* **1959**, 115, 2.

(4) Kugel, K. I.; Khomskii, D. I. *Sov. Phys. Usp.* **1982**, 25, 231.

(5) Tokura, Y.; Nagaosa, N. *Science* **2000**, 288, 462.

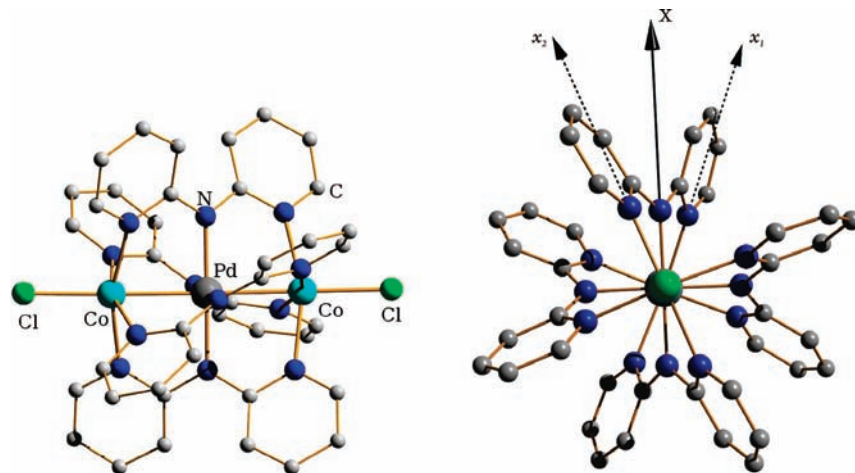


Figure 1. Side and axial views of $[\text{Co}_2\text{PdCl}_2(\text{dpa})_4]$. The dashed lines show the local x axes on the Co sites, while the solid line shows the X axis of the molecular coordinate system.

models have already been applied for several high-symmetry binuclear complexes.^{6–9} Theoretical model studies of the exchange coupling between high-spin Co^{II} ions based on these theories have been reported.^{10,11} In this paper, we apply this theory to explain the magnetism of the $[\text{Co}_2\text{PdCl}_2(\text{dpa})_4]$ complex. On the basis of considerations of the geometry and electronic configuration, a model Hamiltonian is derived and subsequently used to calculate magnetic properties of the complex. With essentially only two parameters, a satisfactory fit of the magnetic susceptibility can be obtained, although it is recognized that the available experimental information does not suffice to assess the correctness of the model completely.

We start with the construction of the model Hamiltonian in the next section, followed by a discussion of its spectrum in some limiting cases in section 3. The application to the title complex is presented in section 4.

2. The Model Hamiltonian

Let us consider the structure of the CoPdCo complex first. The three metal ions are held together in a linear chain by four dipyriddydamido (dpa) ligands that are helically wound around the chain. Two Cl^- ions are coordinated axially to the Co ions. The local symmetry group on the Co sites is C_4 , with the Z axis as shown in Figure 2. Because of the helical nature of the coordinating dpa groups, the local axes on the Co sites are rotated through Z with respect to each other, as shown in Figures 1 and 2. They make an angle of φ with the molecular coordinate system XYZ . Bond distances and magnetic measurements indicate that both Co^{II} ($3d^7$) ions are in the high-spin state ($S = 3/2$), while Pd^{II} ($4d^8$) is in the closed-shell low-spin state ($S = 0$).¹

The octahedral 4T_1 ground states of the two Co^{II} ions will serve as basis functions for the effective Hamiltonian. They are a linear combination of two configurational strong-field states:

$$|{}^4T_1\rangle = c_1|t_2^5e^2{}^4T_1\rangle + c_2|t_2^4e^3{}^4T_1\rangle \quad (2)$$

The contribution of the $t_2^4e^3$ configuration is at most 20% (low-field limit) and goes to 0% in the strong-field limit. Note that the three spatial components of $|{}^4T_1\rangle$ are defined with respect to the local coordinate system on the Co site (see Figure 2). Let $|{}^4T_1^{(i)}\rangle$ denote the 4T_1 state on $\text{Co}(i)$, and then we have

$$\begin{aligned} \text{Co}(1): & \quad \{|{}^4T_1^{(1)}x_1\rangle, |{}^4T_1^{(1)}y_1\rangle, |{}^4T_1^{(1)}z\rangle\} \\ \text{Co}(2): & \quad \{|{}^4T_1^{(2)}x_2\rangle, |{}^4T_1^{(2)}y_2\rangle, |{}^4T_1^{(2)}z\rangle\} \end{aligned} \quad (3)$$

The on-site tetragonal ligand field and spin–orbit coupling are considered to be in the first order of perturbation theory. According to the T–P correspondence, a 4T_1 term can be replaced by a spherical 4P term. For one center, the resulting Hamiltonian is¹⁴

$$\hat{H}_1 = \Delta \left(\hat{L}_{1z}^2 - \frac{2}{3} \right) - \frac{1}{3} \zeta \gamma \hat{L}_1 \cdot \hat{S}_1 \quad (4)$$

where ζ is the spin–orbit coupling constant, γ accounts for the correspondence between the T_1 and P states, and Δ is the tetragonal splitting (Figure 3). The factor γ depends both on the orbital reduction factor κ and on the composition of the 4T_1 states in terms of the $t_2^5e^2$ and $t_2^4e^3$ configurations. It obeys $-3/2\kappa < \gamma < -\kappa$.^{14,15}

We suppose now that the Pd ion can be treated as a ligand in the theory of superexchange interactions, as was the case for diamagnetic metal ions in other trinuclear complexes.¹² This means that states on the Pd ion will not be considered in

(6) Boyd, P. D. W.; Gerloch, M.; Harding, J. H.; Woolley, R. G. *Proc. R. Soc. London, Ser. A* **1978**, *360*, 161.

(7) Ceulemans, A.; Chibotaru, L. F.; Heylen, G. A.; Pierloot, K.; Vanquickenborne, L. G. *Chem. Rev.* **2000**, *100*, 787.

(8) Mironov, V. S.; Chibotaru, L. F.; Ceulemans, A. *J. Am. Chem. Soc.* **2003**, *125*, 9750.

(9) Borrás-Almenar, J. J.; Clemente-Juan, J. M.; Coronado, E.; Palić, A. V.; Tsukerblat, B. S. *J. Phys. Chem. A* **1998**, *102*, 200.

(10) Palić, A. V.; Tsukerblat, B. S.; Coronado, E.; Clemente-Juan, J. M.; Borrás-Almenar, J. J. *J. Chem. Phys.* **2003**, *118*, 5566.

(11) Lloret, F.; Julve, M.; Cano, J.; Ruiz-García, R.; Pardo, E. *Inorg. Chim. Acta* **2008**, *361*, 3432.

(12) Chibotaru, L. F.; Girerd, J.-J.; Blondin, G.; Glaser, T.; Wiegardt, K. *J. Am. Chem. Soc.* **2003**, *125*, 12615.

(13) Liu, I. P.-C.; Lee, G.-H.; Peng, S.-M.; Bénard, M.; Rohmer, M.-M. *Inorg. Chem.* **2007**, *46*, 9602.

(14) Griffith, J. S. *The Theory of Transition-Metal Ions*; Cambridge University Press: Cambridge, U.K., 1964.

(15) Herrera, J. M.; Bleuzen, A.; Dromzée, Y.; Julve, M.; Lloret, F.; Verdaguier, M. *Inorg. Chem.* **2003**, *42*, 7052.

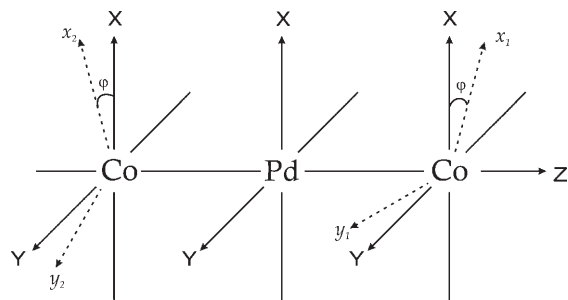


Figure 2. Local coordinate systems x_1y_1z and x_2y_2z on the Co(1) and Co(2) sites, respectively, and the molecular coordinate system XYZ .

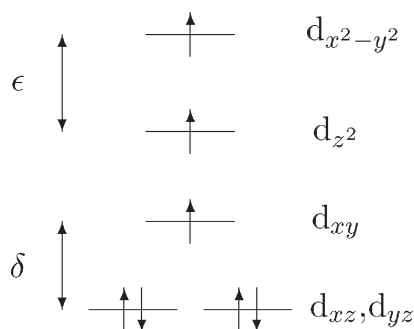


Figure 3. Schematic representation of the $|^4T_{1z}, M_S = 3/2\rangle$ component of the t_2e^2 configuration on Co^{II} . The tetragonal splitting parameter in \hat{H}_1 is given by $\Delta = \delta c_1^2 - [\delta + (3/4)\epsilon]c_2^2$.

the model treatment; the role of the 4d orbitals of Pd is to provide hybridization to the 3d orbitals of Co (and, therefore, pathways for kinetic exchange), a role that is normally played only by nonmetallic ligands. The origin of the strong antiferromagnetic exchange interaction in the present complex can then be understood as follows: in the ground-state configuration of Co^{II} , the $3d_{z^2}$ orbital is singly occupied and has an interaction with the $4d_{z^2}$ orbital on Pd, resulting in a pathway for antiferromagnetic exchange interaction between the spins on the two Co sites.³ The fact that this antiferromagnetic interaction is much stronger than that in conventional dinuclear Co complexes is due to the large spatial extension of 4d orbitals (better σ overlap between d_{z^2} orbitals) and the possibility of near-resonance between the d_{z^2} orbitals on Co and Pd. This interpretation is consistent with the exchange interaction in the isostructural complex $[\text{Cu}_2\text{Pd}(\text{dpa})_4\text{Cl}_2]$, which was found to be much smaller than that in the cobalt compound.¹³ The d_{z^2} orbital on Cu^{II} is indeed doubly occupied, so that the mechanism described above is not available there.

Expressions for the exchange Hamiltonian between corner-shared bioctahedral Co^{II} dimers have been derived within the Anderson kinetic exchange theory by Palii et al.¹⁰ In terms of the kinetic transfer parameter t_σ^3 and an averaged charge-transfer energy U , the Hamiltonian for exchange between the $3d_{z^2}$ orbitals is

$$\hat{H}_{\text{exch},\sigma} = \frac{4}{9} \frac{t_\sigma^2}{U} \left(1 - \frac{3}{4} c_2^2 \hat{L}_{1z}^2\right) \left(1 - \frac{3}{4} c_2^2 \hat{L}_{2z}^2\right) \hat{S}_1 \cdot \hat{S}_2 + \frac{9}{16} c_2^4 \hat{L}_{1z}^2 \hat{L}_{2z}^2 \quad (5)$$

The orbital-dependent anisotropic terms come into $\hat{H}_{\text{exch},\sigma}$ by the fact that, for $|^4T_{1x}\rangle$ and $|^4T_{1y}\rangle$, the $3d_{z^2}$ orbital is, in

part, doubly occupied in the t_2e^3 configuration, therefore reducing the exchange interaction in comparison with $|^4T_{1z}\rangle$. An estimation of c_2^2 can be obtained from the complex $[\text{Co}(\text{NH}_3)_6]^{2+}$, for which $c_2^2 \approx 0.08$.¹⁴ The anisotropic part of $\hat{H}_{\text{exch},\sigma}$, which is $O(c_2^2)$, can thus be considered as a small perturbation on the isotropic Heisenberg Hamiltonian $J_\sigma \hat{S}_1 \cdot \hat{S}_2$. Anticipating the results in section 4, where we will find that the ground state is well separated from the excited states, we can ignore this perturbation without introducing appreciable error in the magnetic susceptibility: at low temperature, only the ground state is occupied, on which the perturbation has little effect, while at higher temperatures, the perturbation becomes irrelevant to the susceptibility.¹⁴

The transfer of π -type (d_{xz} and d_{yz}) and δ -type (d_{xy} and $d_{x^2-y^2}$) electrons can also be mediated by the Pd ion. The corresponding kinetic-transfer parameters t_π and t_δ are progressively smaller than t_σ because, in perturbation theory, they are proportional to the square of the overlap between the Co and Pd orbitals, which is respectively of the π - π and δ - δ types. The smallness of these direct overlaps in comparison with the σ - σ overlap leads us to regard the π - and δ -exchange interactions as small perturbations, which, by the argument of the previous paragraph, can be ignored for the present purpose.

Likewise, several smaller interactions, such as ligand fields of lower symmetry and the Coulomb repulsion between sites, which leads to an energy differentiation akin to exciton dispersion, can be omitted from the Hamiltonian.

In writing down the total Hamiltonian of the dimer in a magnetic field \mathbf{B} , attention must be paid to the fact that the local coordinate axes are not parallel. The cylindrical symmetry of the local and exchange Hamiltonians ensures, however, that, by applying the T-P correspondence

$$\begin{aligned} {}^4P^{(1)}_X &\sim \cos \varphi |^4T_1^{(1)}x_1\rangle + \sin \varphi |^4T_1^{(1)}y_1\rangle \\ {}^4P^{(1)}_Y &\sim -\sin \varphi |^4T_1^{(1)}x_1\rangle + \cos \varphi |^4T_1^{(1)}y_1\rangle \\ {}^4P^{(1)}_Z &\sim |^4T_1^{(1)}Z\rangle \end{aligned} \quad (6)$$

on Co(1) and

$$\begin{aligned} {}^4P^{(2)}_X &\sim \cos \varphi |^4T_1^{(2)}x_2\rangle - \sin \varphi |^4T_1^{(2)}y_2\rangle \\ {}^4P^{(2)}_Y &\sim \sin \varphi |^4T_1^{(2)}x_2\rangle + \cos \varphi |^4T_1^{(2)}y_2\rangle \\ {}^4P^{(2)}_Z &\sim |^4T_1^{(2)}Z\rangle \end{aligned} \quad (7)$$

on Co(2), the total effective Hamiltonian, written in the molecular coordinate system XYZ (Figure 2), is independent of the angle φ :

$$\begin{aligned} \hat{H} &= \Delta \left(\hat{L}_{1z}^2 + \hat{L}_{2z}^2 - \frac{4}{3} \right) - \frac{1}{3} \xi \gamma (\hat{L}_1 \cdot \hat{S}_1 + \hat{L}_2 \cdot \hat{S}_2) \\ &+ J_\sigma \hat{S}_1 \cdot \hat{S}_2 + \mu_B [2(\hat{S}_1 + \hat{S}_2) + \gamma(\hat{L}_1 + \hat{L}_2)] \cdot \mathbf{B} \end{aligned} \quad (8)$$

working in the space of $|\text{LSM}_L M_S\rangle_1 \cdot |\text{LSM}_L M_S\rangle_2$ states ($L = 1$ and $S = 3/2$), which are defined in the same XYZ coordinate system. We remark here that the obtained exchange Hamiltonian ($J_\sigma \hat{S}_1 \cdot \hat{S}_2$) is the isotropic Heisenberg interaction between real spins, which was tentatively introduced by Lines in a model for the thermodynamic properties of Co clusters.¹⁶ The above derivation confirms the

(16) Lines, M. E. *J. Chem. Phys.* **1971**, *55*, 2977.

correctness of Lines' model for the present compound but underlines at the same time the fact that this correctness is not trivial and cannot be expected to hold in every case.

Before applying Hamiltonian (8) to the problem at hand, we will consider some properties of its spectrum.

3. Exchange Spectrum in Some Limiting Cases

To gain a better insight into the meaning of the Hamiltonian in eq 8, it is useful to consider some special cases that are covered by this Hamiltonian in a zero magnetic field. The most convenient approach is to start from the spectrum of the single Co^{II} ions, described by the Hamiltonian in eq 4. Because this Hamiltonian has cylindrical symmetry around the z axis, the eigenstates are labeled by a rotational quantum number M_J , with the pairs $\pm M_J$ being degenerate (Kramers degeneracy). A plot of the energy levels as a function of Δ is presented in Figure 4. Three limiting regimes are apparent: $\Delta/|\gamma\zeta| \gg 1$, $= 0$, and $\ll -1$. In each of these, the lowest states of the dimer can be described by a Hamiltonian of lower dimension if the exchange interaction is much smaller than the intrasite interactions.

Consider first the case where Δ is positive and large and the ground state is a spin-only state (${}^4\text{A}$ in the point group C_4), corresponding to the electron configuration drawn in Figure 3. In this space, the effective Hamiltonian has the form of the well-known spin Hamiltonian in eq 1:

$$\hat{H} = J\hat{S}_1 \cdot \hat{S}_2 + D(\hat{S}_{1z}^2 + \hat{S}_{2z}^2) \quad (9)$$

with $J = J_\sigma$, $D = \gamma^2\zeta^2/9\Delta$, and $S_1 = S_2 = 3/2$. The exchange interaction retains the isotropic form, while the effect of spin-orbit coupling is a positive zero-field splitting.

For the second case, we set $\Delta = 0$. The intrasite Hamiltonian equation (4) now has spherical symmetry. The eigenstates correspond to quantum numbers of total angular momentum $J = 5/2, 3/2$, and $1/2$, separated according to the Landé interval rule. The ground state is the doublet $J = 1/2$ (Figure 4). If we assign to this state an effective spin, $\tilde{s} = 1/2$, and evaluate the exchange interaction to first order, we obtain the exchange Hamiltonian in a four-dimensional space:

$$\hat{H} = J\hat{S}_1 \cdot \hat{S}_2 \quad (10)$$

where $J = (25/9)J_\sigma$, as one can find from the Landé g factor. Again, the isotropic form of the exchange coupling is retained, although in another space.

In the third case, Δ is large and negative, whereby the ground state has orbital momentum along the z axis (${}^4\text{E}$ in the point group C_4). Spin-orbit coupling splits this state into four equidistant doublets (Figure 4), the lowest of which consists of the states $|M_L M_S\rangle = |-1 \ 3/2\rangle$ and $|1 \ -3/2\rangle$. These are assigned as respectively $\tilde{s}_z = +1/2$ and $\tilde{s}_z = -1/2$ components of an effective $\tilde{s} = 1/2$ spin. The exchange Hamiltonian is found to be (again in a four-dimensional space)

$$\hat{H} = J\hat{S}_{1z}\hat{S}_{2z} \quad (11)$$

with $J = 9J_\sigma$. In contrast to the previous case (eq 10), this Hamiltonian is of the anisotropic Ising type. In general, for $\Delta < 0$, the exchange Hamiltonian will be a linear combination of an isotropic (eq 10) and an anisotropic (eq 11) part.

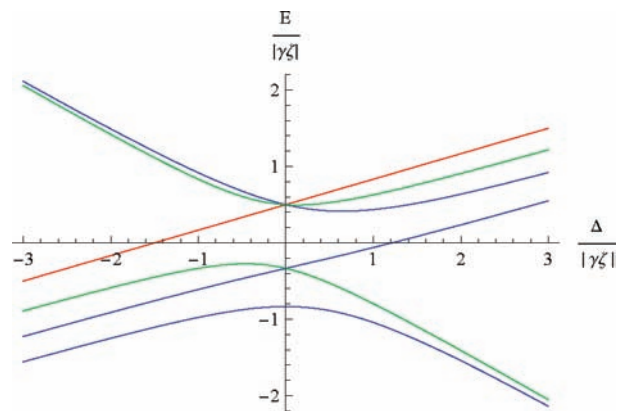


Figure 4. Spectrum of the uncoupled Co^{II} ions [Hamiltonian equation (4)] as a function of the tetragonal splitting Δ . (Adapted from ref 14.) The ${}^4\text{T}_1$ ground state is split by spin-orbit coupling and a tetragonal ligand field in six Kramers doublets, each of which is represented by a single line in the figure. States are identified by the rotational quantum number M_J : blue, $M_J = \pm 1/2$; green, $M_J = \pm 3/2$; red, $M_J = \pm 5/2$.

The parent Hamiltonian equation (8) contains thus as limiting cases a variety of interactions in a more familiar form, ranging from isotropic spin-spin coupling with zero-field splitting to the anisotropic Ising Hamiltonian. We want to emphasize again that, for these derivations, the exchange interaction was supposed to be small with respect to the interactions on the single Co sites. Only then can the lowest eigenstates of each Co site form a good model space for an exchange Hamiltonian with reduced dimensions. We will find in the next section that such an approximation cannot be made for the $[\text{Co}_2\text{PdCl}_2(\text{dpa})_4]$ complex so that a spin-only Hamiltonian, as was used in ref 1, is not adequate here.

4. Magnetic Susceptibility of $[\text{Co}_2\text{PdCl}_2(\text{dpa})_4]$

Properties dependent on the temperature are calculated by diagonalizing Hamiltonian equation (8) and applying Boltzmann statistics. The spin-orbit coupling constant ζ is taken to be 500 cm^{-1} .¹⁴ The three unknowns that are left (Δ , γ , and J_σ) should be determined from a comparison with experiment, remembering the restriction on γ discussed in section 2.

The procedure is applied to the average magnetic susceptibility of $[\text{Co}_2\text{PdCl}_2(\text{dpa})_4]$, for which experimental data are available.¹ The best correspondence is obtained with the following parameters (these parameters were not determined by a least-squares fitting but only by a visual comparison; a more precise fitting is unnecessary for the present purpose):

$$|\Delta| = 100 \text{ cm}^{-1}, \quad J_\sigma = 100 \text{ cm}^{-1}, \quad \gamma = -1.1 \quad (12)$$

The corresponding plots of χ and χT are presented in Figure 5, together with the experimental curves. The value found for γ is typical for high-spin Co^{II} complexes.^{11,15} We should note here that the effect of changing γ was found to be merely a shift of χ , almost independent of the temperature. The essential form of χ depends thus on the values of J_σ and Δ alone. The exchange constant J_σ is strongly antiferromagnetic, as we expected (see section 2). On the other hand, the tetragonal ligand-field splitting Δ is smaller than expected, considering the highly heterogeneous coordination environment of the Co ions. The sign of Δ will be commented on later.

From Figure 5, it is clear that the calculated χ values at low temperature are incompatible with the steep increase of the

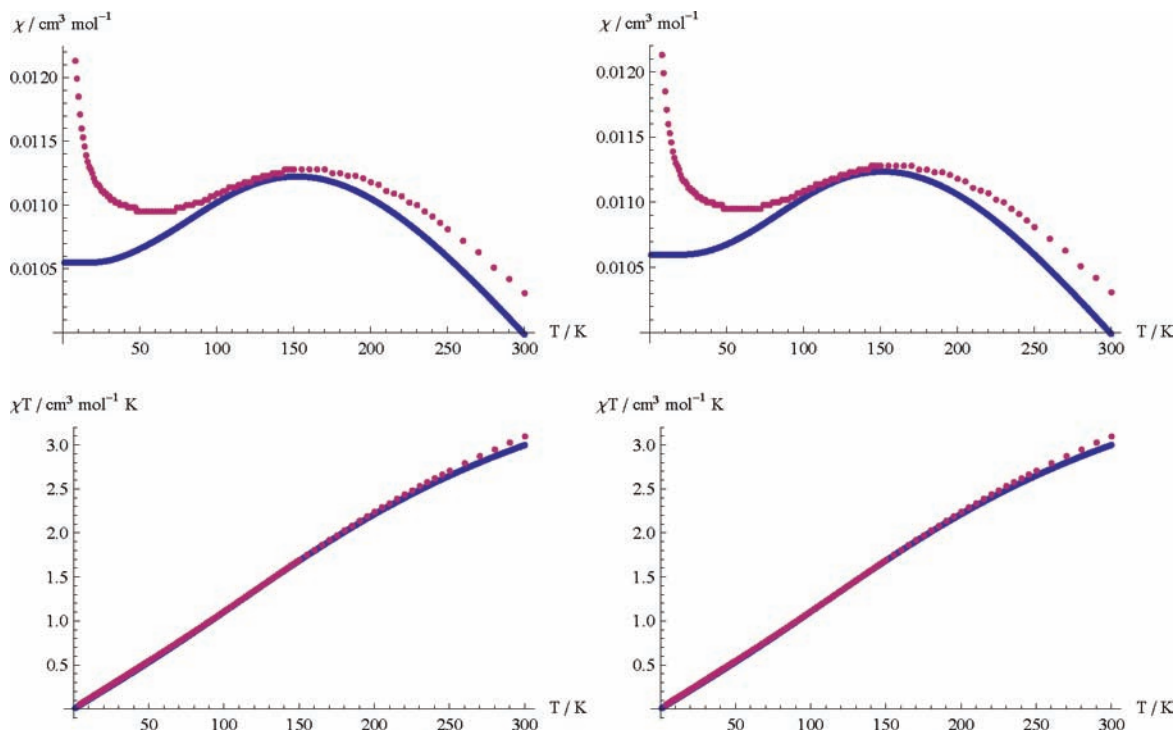


Figure 5. Calculated (blue) and experimental¹ (red) magnetic susceptibility curves of $[\text{Co}_2\text{PdCl}_2(\text{dpa})_4]$ as a function of the temperature. Left: calculated for $\Delta = +100 \text{ cm}^{-1}$. Right: calculated for $\Delta = -100 \text{ cm}^{-1}$. The sign of Δ cannot be determined from this comparison. The calculated susceptibility confirms that the steep increase of the experimental susceptibility below 50 K has to be attributed to a paramagnetic impurity in the sample¹ ($J_o = 100 \text{ cm}^{-1}$, $\zeta = 500 \text{ cm}^{-1}$, and $\gamma = -1.1$).

experimental χ and support thereby the conclusion that this increase is due to a paramagnetic impurity in the sample.¹ The most important result, however, is to be inferred from the curves of χT in Figure 5; the linearity of χT points to a strong temperature-independent paramagnetism (TIP) in the compound, extending over the whole temperature range. This behavior is recovered completely by the theoretical model. The value of the TIP in this compound is about $0.01 \text{ cm}^3 \text{ mol}^{-1}$, which is 100 times larger than common values in mononuclear complexes.¹⁷

To clarify the TIP behavior, we refer to a plot of the energy levels in Figure 6. The three lowest levels, one of which is 2-fold degenerate, are clearly separated from higher levels. In the range of temperatures considered here (below 300 K), only these three ground-state levels are populated appreciably, and their properties will therefore determine the observed magnetism.

A qualitative understanding of the origin of these states can be gained by considering the limit of the weak exchange coupling (J_o small). With $|\Delta| = 100 \text{ cm}^{-1}$, we are in a regime very close to the octahedral limit (center of Figure 4). According to the discussion in section 3, an effective Hamiltonian can be written that couples the ground-state Kramers doublets on each Co site:

$$\hat{H} = J_a \hat{\mathbf{s}}_1 \cdot \hat{\mathbf{s}}_2 + J_b \hat{s}_{1z} \hat{s}_{2z} \quad (13)$$

The J_a term couples the doublets spherically in a triplet state and a singlet ground state (the exchange is still anti-ferromagnetic). The J_b term results from the deviation from octahedral symmetry and splits the triplet in rotational

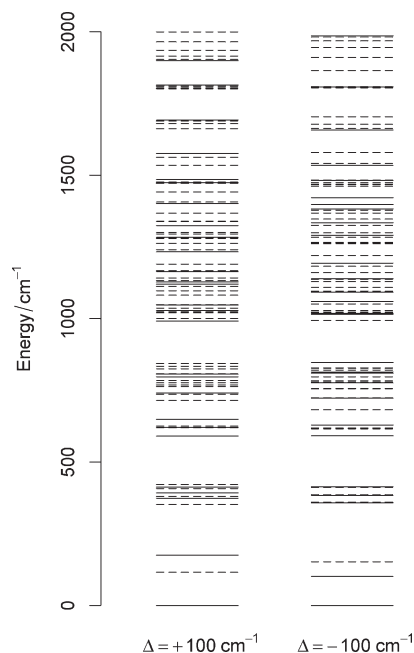


Figure 6. Energy levels of the model Hamiltonian (8) in a zero magnetic field. Full lines represent nondegenerate levels, and dashed lines represent 2-fold degenerate levels ($J_o = 100 \text{ cm}^{-1}$, $\zeta = 500 \text{ cm}^{-1}$, and $\gamma = -1.1$).

components $m_{\bar{s}} = 0$ and $m_{\bar{s}} = \pm 1$. A perturbational approach shows that¹⁰ $J_b = -(40/9)(\Delta/|\gamma\zeta|)J_o$. This expression, which is correct in the weak exchange limit, predicts that the relative order of the second and third levels depends on the sign of Δ . This same ordering is found in the present case of strong exchange coupling (Figure 6). At least formally then, the lowest energy levels can be described by the

(17) Kahn, O. *Molecular Magnetism*; VCH Publishers: New York, 1993.

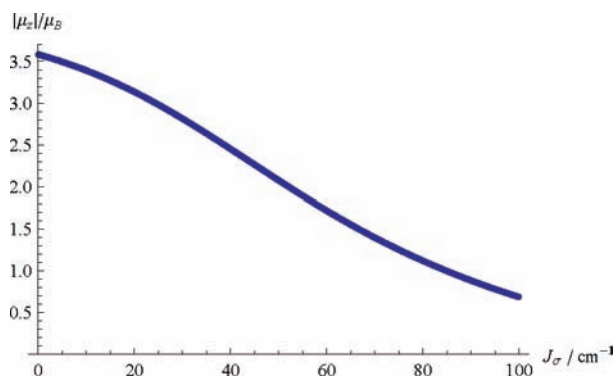


Figure 7. z component of the magnetic moment of the lowest 2-fold degenerate state of Hamiltonian (8) in a zero magnetic field, as a function of the antiferromagnetic exchange interaction ($\Delta = +100 \text{ cm}^{-1}$, $\zeta = 500 \text{ cm}^{-1}$, and $\gamma = -1.1$).

Hamiltonian (13), although the composition of the states is certainly not the one implied by the weak coupling limit: the strong exchange interaction ($J_\sigma \hat{S}_1 \cdot \hat{S}_2$) will mix the ground-state Kramers doublets on the Co sites to an important extent with higher doublets. The model space of Hamiltonian (13), consisting only of the ground-state Kramers doublets, is therefore incapable of representing the real states accurately. In this respect, the effective Hamiltonian (13) is not considered to be appropriate for the present system.

To exemplify the deviation from the weak coupling limit, we consider the z component (because of the symmetry of the molecule, x and y components of the magnetic moment vanish in every state) of the magnetic moment in the 2-fold degenerate level ($m_s = \pm 1$). Figure 7 shows how this moment decreases with an increase in the strength of the exchange interaction: from $3.6 \mu_B$ at $J_\sigma = 0 \text{ cm}^{-1}$ (that is, for two independent Co ions) to $0.7 \mu_B$ at $J_\sigma = 100 \text{ cm}^{-1}$, a quenching that is to be attributed to the tendency of the antiferromagnetic exchange interaction to align the spin moments antiparallel (and, through spin-orbit coupling, also the orbital moments). The strong reduction of this magnetic moment is part of the explanation of the TIP behavior, to which we come now.

The magnetic properties of the lowest levels are most conveniently analyzed with the help of the Van Vleck equation, which expresses the susceptibility in terms of the zero-field molecular states:

$$\chi = \frac{1}{3} \sum_{\alpha=x,y,z} \frac{N_A}{\sum_n g_n e^{-\epsilon_n/kT}} \times \sum_n \left(\sum_{i,j \in \{n\}} \frac{|\langle n_i | \hat{\mu}_\alpha | n_j \rangle|^2}{kT} + 2 \sum_{m \neq n} \sum_{i \in \{n\}} \sum_{j \in \{m\}} \frac{|\langle n_i | \hat{\mu}_\alpha | m_j \rangle|^2}{\epsilon_m - \epsilon_n} \right) e^{-\epsilon_n/kT} \quad (14)$$

The term between brackets denotes the susceptibility of one level $\{n\}$ with degeneracy g_n and energy ϵ_n . It is a sum of two parts: the first is due to *permanent* magnetic moments in the level and is inversely proportional to temperature (note that permanent magnetic moments are only possible in degenerate levels, i.e., for $g_n \geq 2$); the second part is due to magnetic moments that are *induced* by the magnetic field. TIP is usually due to the latter part, when only the ground state is thermally

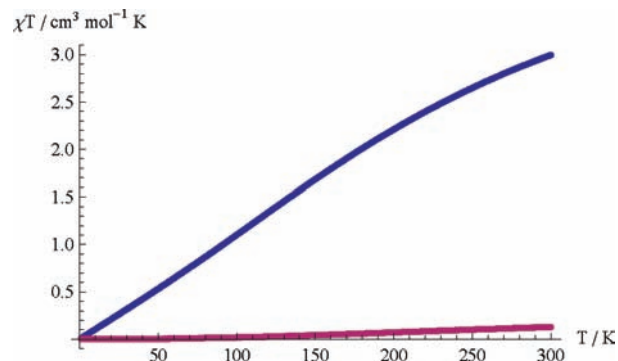


Figure 8. Contributions to the calculated magnetic susceptibility. The blue curve is the total χT , and the red curve is the part of χT due to permanent magnetic moments. The difference equals the contribution of the induced magnetic moments ($\Delta = +100 \text{ cm}^{-1}$, $J_\sigma = 100 \text{ cm}^{-1}$, $\zeta = 500 \text{ cm}^{-1}$, and $\gamma = -1.1$).

occupied.¹⁷ In the present case, however, we have seen that two more levels can be populated, one of which is 2-fold degenerate. The fact that the TIP is hardly affected by these states is explained by two observations: First, the susceptibility due to induced magnetic moments is almost the same in these levels and has a value of $\approx 0.01 \text{ cm}^3 \text{ mol}^{-1}$. Second, the permanent magnetic moment in the degenerate level is small ($\approx 0.7 \mu_B$; see Figure 7). At the temperatures where this level becomes populated, the contribution of this moment to the susceptibility is small in comparison with the $0.01 \text{ cm}^3 \text{ mol}^{-1}$ value of the induced moments; it does contribute to the maximum of χ at 150 K, which is only about 7% higher than the value at 0 K (Figure 5). In the χT curve, this deviation is hardly noticed. We understand here that the quenching of the magnetic moment in the degenerate level, as described in the previous paragraph, is essential for the manifestation of the TIP behavior. Overall, we conclude that the magnetic susceptibility is dominated by the contribution of the induced magnetic moments, which are equal in the thermally occupied states, resulting in a temperature-independent behavior. Figure 8 illustrates that the contribution of the induced magnetic moments is by far the most important: the susceptibility due to the permanent moments (red curve) is very small in comparison with the total susceptibility (blue curve).

It is important to note that the large TIP cannot solely be attributed to the coupling of the Co^{II} ions. In fact, a TIP contribution of the same order of magnitude is already present in free, octahedral high-spin Co^{II} complexes. There, χT is linear up to $\approx 100 \text{ K}$ and flattens at higher temperatures because of population of the $J = 3/2$ level.¹¹ The origin of this TIP is the induced magnetic moments in the ground-state $J = 1/2$ level. The peculiarity of the present dimer lies in the fact that the TIP behavior is extended over the whole experimental temperature range, making it more manifest.

As was indicated in eq 12, the sign of Δ could not be determined from a comparison with experiment. This is clear from Figure 5, where we show the calculated curves for positive Δ on the left and those for negative Δ on the right. A differentiation between both cases can only be made by looking at the components of χ along the molecular Z axis and perpendicular to it, as shown in Figure 9, where the calculated components are plotted for both signs of Δ . The magnetic anisotropy ($\chi_{\parallel} - \chi_{\perp}$) is clearly dependent on the sign of Δ , although the average susceptibility $\chi = (\chi_{\parallel} + 2\chi_{\perp})/3$ does not change. Note that, for $\Delta = -100 \text{ cm}^{-1}$, the

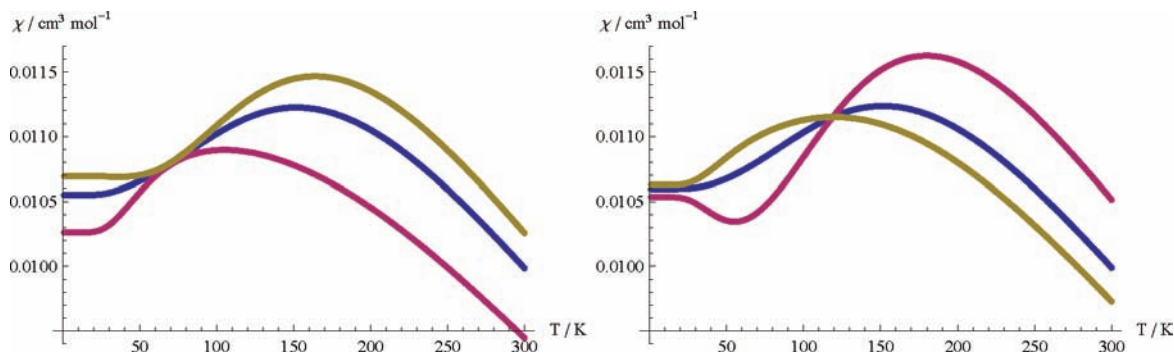


Figure 9. Calculated components of magnetic susceptibility: χ_{\parallel} (red), χ_{\perp} (yellow), and χ (blue). Left: $\Delta = +100 \text{ cm}^{-1}$. Right: $\Delta = -100 \text{ cm}^{-1}$. ($J_{\sigma} = 100 \text{ cm}^{-1}$, $\zeta = 500 \text{ cm}^{-1}$, and $\gamma = -1.1$.)

anisotropy is also predicted to change sign as a function of the temperature. Unfortunately, there are no experimental data to confront these predictions with. Oriented crystal measurements on this compound would provide information that could lead to a more decisive test of the theoretical model.

5. Conclusion

From a microscopic approach to the electronic structure of $[\text{Co}_2\text{PdCl}_2(\text{dpa})_4]$, we have derived a model Hamiltonian that takes into account both the spin and orbital degeneracy of the Co^{II} ions. By considering the nonmagnetic Pd^{II} ion as a ligand that transfers exchange interaction between the Co^{II} ions, the dominant contribution to the exchange Hamiltonian was found to be of the isotropic Heisenberg type between real spins. The calculated magnetic susceptibility shows a satisfactory agreement with experiment. In particular, the strong TIP is recovered completely (Figure 5). The parameters derived from this comparison confirm that the Co ions are coupled by a strong antiferromagnetic exchange interaction.¹ The tetragonal ligand-field splitting was found to be small ($|\Delta| = 100 \text{ cm}^{-1}$), and its sign could not be determined from the available experimental data.

The observed TIP in this complex results from a quenching of permanent magnetic moments together with an almost constant magnetic polarizability in thermally populated levels. This should

be contrasted with the usual origin of TIP, which is a non-magnetic ground state, thermally isolated from excited states.

It should be emphasized that to explain the magnetism of this compound, a conventional spin-only Hamiltonian is not appropriate. The relative strength of the interactions do not allow for a reduction of the size of the model space. The lack of a generic spin-Hamiltonian approach remains a major problem in the study of magnetic compounds with unquenched orbital momenta.

Although Co^{II} is known for its highly anisotropic behavior, this property does not emerge in the compound studied in this paper. The reason is that Δ , which is the only parameter in eq 8 that induces anisotropy, is too small: its effect is quenched by the strong exchange interaction, which is isotropic (eq 8). To obtain strong magnetic anisotropy, Δ should be made large and negative. On the other hand, if the σ -exchange pathway can be eliminated by a suitable choice of ligands while retaining the π -exchange pathway, the exchange Hamiltonian will be anisotropic, and the Heisenberg Hamiltonian will be inadequate.

Acknowledgment. We thank I. P.-C. Liu and Dr. S.-M. Peng for making the magnetic susceptibility data available.¹ We thank Dr. Marc Bénard and Dr. Marie-Madeleine Rohmer for useful discussions. W.V.d.H. is “Aspirant van het FWO”.